Direct computation of light quarks and strange helicity PDFs with lattice QCD

Floriano Manigrasso

University of Cyprus University of Rome "Tor Vergata"
Humboldt University of Berlin

In collaboration with:
Constantia Alexandrou, Martha Constantinou,
Kyriakos Hadjyiannakou

2020 Meeting on Lattice Parton Physics from Large-Moment Effective Theory (LaMET2020)
September 7-11, 2020

STIMULATE
European Joint Doctorates

Overview

Helicity PDFs

In a longitudinally polarized proton, probability of finding a quark with momentum fraction x and spin parallel to that of the parent nucleon

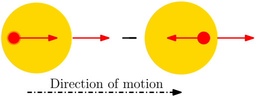

Overview

Helicity PDFs

In a longitudinally polarized proton, probability of finding a quark with momentum fraction x and spin parallel to that of the parent nucleon

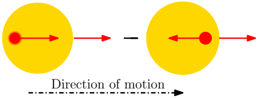

- Together with unpolarized and transversity PDFs, the helicity PDFs play a key role in the on-going experimental program of major facilities BNL, CERN, DESY, Fermilab, JLab and SLAC;

Overview

Helicity PDFs

In a longitudinally polarized proton, probability of finding a quark with momentum fraction x and spin parallel to that of the parent nucleon

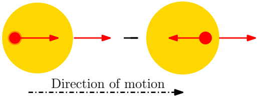

- Together with unpolarized and transversity PDFs, the helicity PDFs play a key role in the on-going experimental program of major facilities BNL, CERN, DESY, Fermilab, JLab and SLAC;
- Accessed experimentally in deep-inelastic scattering (DIS), semi-inclusive DIS, Drell-Yan, and proton-proton scattering processes;

Overview

Helicity PDFs

In a longitudinally polarized proton, probability of finding a quark with momentum fraction *x* and spin parallel to that of the parent nucleon

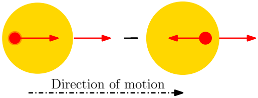

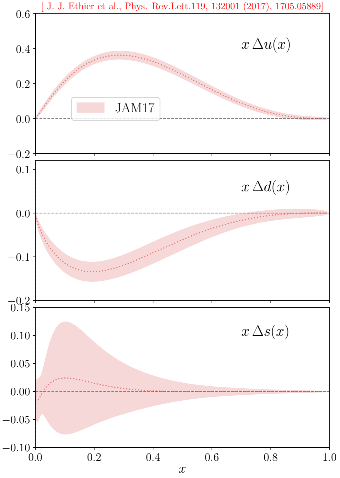

- Together with unpolarized and transversity PDFs, the helicity PDFs play a key role in the on-going experimental program of major facilities BNL, CERN, DESY, Fermilab, JLab and SLAC;
- Accessed experimentally in deep-inelastic scattering (DIS), semi-inclusive DIS, Drell-Yan, and proton-proton scattering processes;
- Strange PDF is entirely unconstrained from DIS data, it improves with the inclusion of kaon production SIDIS data;

[M. Constantinou et al. (2020), 2006.08636]

Table of contents

Quasi-PDF approach 1/2

[X. Ji, Phys. Rev. Lett. 110 (2013) 262002 [arXiv:1305.1539]]

- The quasi-PDFs are defined in momentum space

$$\widetilde{\Delta}q(x,\mu,P) = 2P_3 \int_{-\infty}^{+\infty} \frac{dz}{4\pi}\, e^{-ixP_3 z}\, \mathcal{M}^R(z,P_3)\,,$$

Quasi-PDF approach 1/2

[X. Ji, Phys. Rev. Lett. 110 (2013) 262002 [arXiv:1305.1539]]

- The quasi-PDFs are defined in momentum space

$$\widetilde{\Delta} q(x,\mu,P) = 2P_3 \int_{-\infty}^{+\infty} \frac{dz}{4\pi}\, e^{-ixP_3 z}\, \mathcal{M}^R(z,P_3)\,,$$

- Fourier transform of hadronic matrix elements

$$\mathcal{M}^R(z,P_3,\mu) \equiv Z(z,\mu)\,\mathcal{M}(z,P_3)\,,$$

$$\mathcal{M}(z,P_3) \equiv \langle N(P)|\overline{\psi}(z)\gamma^3\gamma^5 W(0,z)\psi(0)\,|N(P)\rangle,\ \psi = \begin{pmatrix} u \\ d \end{pmatrix} \text{ or } \psi = s$$

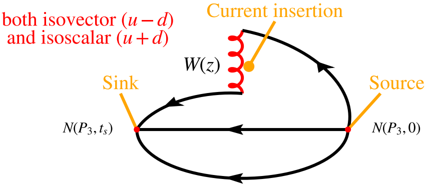

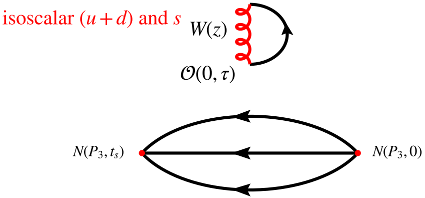

Quasi-PDF approach 1/2

[X. Ji, Phys. Rev. Lett. 110 (2013) 262002 [arXiv:1305.1539]]

- The quasi-PDFs are defined in momentum space

$$\widetilde{\Delta q}(x, \mu, P) = 2P_3 \int_{-\infty}^{+\infty} \frac{dz}{4\pi} e^{-ixP_3 z} \mathcal{M}^R(z, P_3),$$

- Fourier transform of hadronic matrix elements

$$\mathcal{M}^R(z, P_3, \mu) \equiv Z(z, \mu) \mathcal{M}(z, P_3),$$

$$\mathcal{M}(z, P_3) \equiv \langle N(P)|\overline{\psi}(z)\gamma^3\gamma^5 W(0, z)\psi(0)|N(P)\rangle, \ \psi = \begin{pmatrix} u \\ d \end{pmatrix} \text{ or } \psi = s$$

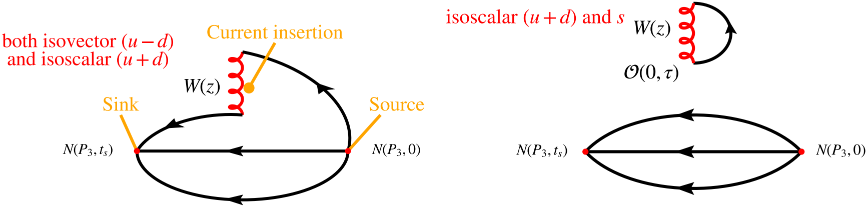

Disconnected contributions much more difficult and expensive to compute!

require the use of appropriate stochastic and gauge-noise reduction techniques

Quasi-PDF approach 2/2

- Evaluation of the renormalization functions $Z(z, \mu)$ in the intermediate $\mathrm{RI-MOM}$ scheme at μ_0 and conversion to $\mathrm{M\overline{MS}}$ at $\mu = 2\,\mathrm{GeV}$;

  [C. Alexandrou Phys. Rev.D99, 114504 (2019), 1902.00587]

Quasi-PDF approach 2/2

- Evaluation of the renormalization functions $Z(z, \mu)$ in the intermediate $\mathrm{RI} - \mathrm{MOM}$ scheme at μ_0 and conversion to $\mathrm{M\overline{MS}}$ at $\mu = 2\,\mathrm{GeV}$;

  [C. Alexandrou Phys. Rev.D99, 114504 (2019), 1902.00587]

- Quasi-PDFs differ from light-cone PDFs by $\mathcal{O}\left(\Lambda^2_{\mathrm{QCD}}/P_3^2, m_N^2/P_3^2\right)$. This difference can be evaluated in continuum perturbation theory within Large Momentum Effective Theory (LaMET)

$$\Delta q(x,\mu) = \int_{-\infty}^{\infty} \frac{d\xi}{|\xi|}\, C\left(\xi, \frac{\mu}{xP_3}\right) \widetilde{\Delta q}\left(\frac{x}{\xi}, \mu, P_3\right)$$

  - we employ the one loop matching procedure for the non-singlet case

Quasi-PDF approach 2/2

- Evaluation of the renormalization functions $Z(z, \mu)$ in the intermediate $\mathrm{RI}-\mathrm{MOM}$ scheme at μ_0 and conversion to $\mathrm{M}\overline{\mathrm{MS}}$ at $\mu = 2\,\mathrm{GeV}$;

  [C. Alexandrou Phys. Rev.D99, 114504 (2019), 1902.00587]

- Quasi-PDFs differ from light-cone PDFs by $\mathcal{O}\left(\Lambda^2_{\mathrm{QCD}}/P_3^2, m_N^2/P_3^2\right)$. This difference can be evaluated in continuum perturbation theory within Large Momentum Effective Theory (LaMET)

$$\Delta q(x,\mu) = \int_{-\infty}^{\infty} \frac{d\xi}{|\xi|}\, C\left(\xi, \frac{\mu}{xP_3}\right) \widetilde{\Delta} q\left(\frac{x}{\xi}, \mu, P_3\right)$$

  - we employ the one loop matching procedure for the non-singlet case

- Last step consists of applying the Nucleon Mass Corrections (NMCs) to correct for $m_N/P_3 \neq 0$ in a finite momentum frame

  [J.W. Chen et al., Nucl.Phys. B911 (2016) 246-273,arXiv:1603.06664 [hep-ph]]

Table of contents

Computation of disconnected diagrams

The disconnected quark loop with Wilson line reads

$$\mathcal{L}(t_{\rm ins}, z) = \sum_{\vec{x}_{\rm ins}} \mathrm{Tr}\left[D_q^{-1}(x_{\rm ins}; x_{\rm ins}+z)\gamma^3\gamma^5 W(x_{\rm ins}, x_{\rm ins}+z)\right]$$

Algorithm

- we computed first $N_{ev} = 200$ eigen-pairs of the squared Dirac twisted-mass operator
- stochastic evaluation of the high-modes contribution to the all-to-all propagator
  - to reduce the contamination of the off diagonal terms up to a coloring distance 2^k ($k = 3$) we employ the hierarchical probing algorithm;
    [A. Stathopoulos et al., 1302.4018]
  - in addition, we make use of the one-end trick;
    [UKQCD, M. Foster and C. Michael, Phys. Rev.D59,074503 (1999), hep-lat/9810021]
    [UKQCD, C. McNeile and C. Michael, Phys. Lett.B556,177 (2003), hep-lat/0212020]
  - fully dilute spin and color subspaces.

We have employed such methods in many recent studies:
[C. Alexandrou et al., (2019), 1909.00485]
[C. Alexandrou et al., (2020), 2003.08486]
[C. Alexandrou et al., (2019) 1909.10744]

[C. Alexandrou et al., Phys. Rev.D100, 014509(2019), 1812.10311]

Numerical setup and statistics

Gauge ensemble with $N_f = 2 + 1 + 1$ twisted mass fermions produced by the Extended Twisted Mass Collaboration

[C. Alexandrou et al., Phys. Rev.D98, 054518 (2018),1807.00495]

$32^3 \times 64$	a=0.0938(3)(2) fm	$m_N = 1.050(8)$ GeV
$L = 3.0$ fm	$m_\pi \approx 260$ MeV	$m_\pi L \approx 4.0$

Numerical setup and statistics

Gauge ensemble with $N_f = 2 + 1 + 1$ twisted mass fermions produced by the Extended Twisted Mass Collaboration

[C. Alexandrou et al., Phys. Rev.D98, 054518 (2018),1807.00495]

$32^3 \times 64$	a=0.0938(3)(2) fm	$m_N = 1.050(8)$ GeV
$L = 3.0$ fm	$m_\pi \approx 260$ MeV	$m_\pi L \approx 4.0$

Statistics disconnected diagrams

	Loops					2pt functions		
P_3 [GeV]	N_{ev}	N_{conf}	N_{Had}	N_{sc}	N_{inv}	N_{srcs}	N_{dir}	N_{meas}
0.41	200	330	512	12	$\sim 6k$	200	6	$396k$
0.83	200	330	512	12	$\sim 6k$	200	6	$396k$
1.24	200	480	512	12	$\sim 6k$	200	6	$576k$

at $P_3 = 1.24\,\mathrm{GeV}$ total number of measurements $N_{meas} \sim 2M$

Numerical setup and statistics

Gauge ensemble with $N_f = 2+1+1$ twisted mass fermions produced by the Extended Twisted Mass Collaboration

[C. Alexandrou et al., Phys. Rev.D98, 054518 (2018),1807.00495]

$32^3 \times 64$	a=0.0938(3)(2) fm	$m_N = 1.050(8)$ GeV
$L = 3.0$ fm	$m_\pi \approx 260$ MeV	$m_\pi L \approx 4.0$

Statistics disconnected diagrams

	Loops					2pt functions		
P_3 [GeV]	N_{ev}	N_{conf}	N_{Had}	N_{sc}	N_{inv}	N_{srcs}	N_{dir}	N_{meas}
0.41	200	330	512	12	$\sim 6k$	200	6	$396k$
0.83	200	330	512	12	$\sim 6k$	200	6	$396k$
1.24	200	480	512	12	$\sim 6k$	200	6	$576k$

at $P_3 = 1.24\,\mathrm{GeV}$ total number of measurements $N_{meas} \sim 2M$

Statistics connected diagrams

P_3 [GeV]	N_{conf}	N_{src}	N_{meas}	t_s [fm]
0.41	50	8	400	0.94
0.83	194	8	1552	1.13
1.24	395	16	6320	1.13

Table of contents

Matrix elements

Calculation of matrix elements with boosted hadrons

$$C_{2pt} = \langle \Omega | N(P) \overline{N}(P) | \Omega \rangle \quad C_{3pt} = \langle \Omega | N(P) O(\tau; z) \overline{N}(P) | \Omega \rangle$$

$$O(\tau; z) = \overline{\psi}(z) \gamma^3 \gamma^5 W(0, z) \psi(0)$$

evaluate ratios

$$C_{3pt}(t_s, \tau, P_3) / C_{2pt}(t_s, P_3) \overset{0 \ll \tau \ll t_s}{=} \mathcal{M}(z, P_3)$$

Study of the excited states contamination $t_s = 0.75, 0.84, 0.94, 1.03, 1.13\,\mathrm{fm}$

Matrix elements

Calculation of matrix elements with boosted hadrons

$$C_{2pt} = \langle \Omega | N(P) \overline{N}(P) | \Omega \rangle \quad C_{3pt} = \langle \Omega | N(P) O(\tau; z) \overline{N}(P) | \Omega \rangle$$

$$O(\tau; z) = \overline{\psi}(z) \gamma^3 \gamma^5 W(0, z) \psi(0)$$

evaluate ratios

$$C_{3pt}(t_s, \tau, P_3) / C_{2pt}(t_s, P_3) \overset{0 \ll \tau \ll t_s}{=} \mathcal{M}(z, P_3)$$

Study of the excited states contamination $t_s = 0.75, 0.84, 0.94, 1.03, 1.13\,\mathrm{fm}$

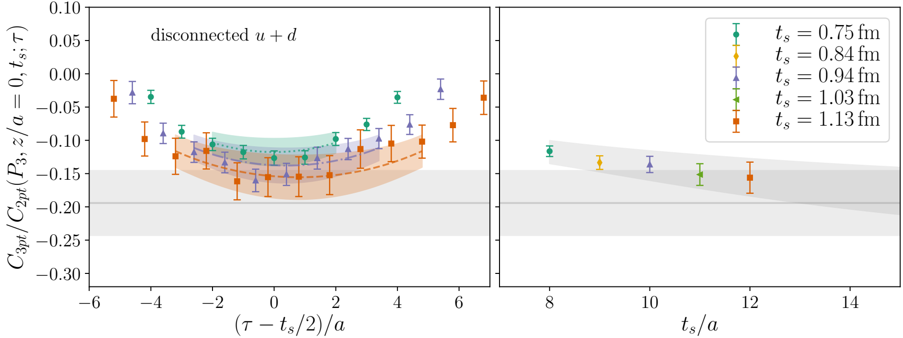

In what follows we use plateau fit results at $t_s = 1.13\,\mathrm{fm}$

Contributions to the isoscalar matrix elements

Momentum dependence

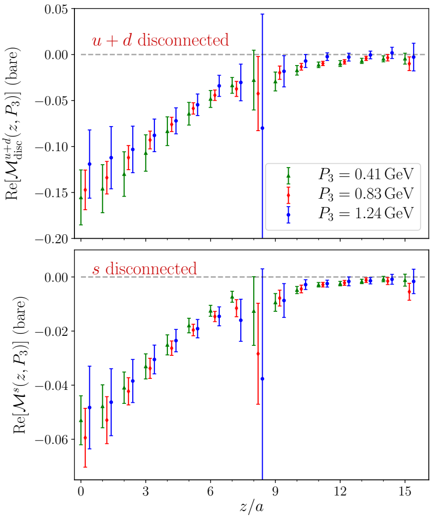

Contributions to the isoscalar matrix elements

Momentum dependence

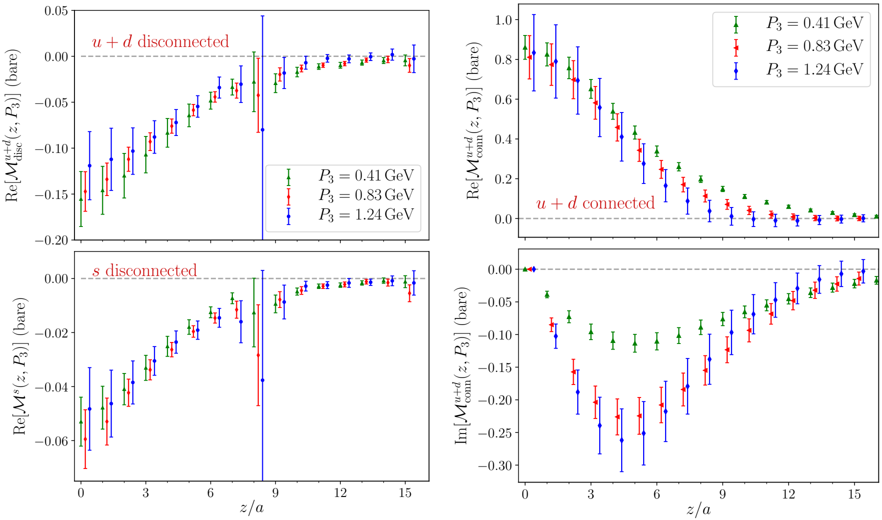

Renormalized matrix elements

Momentum dependence

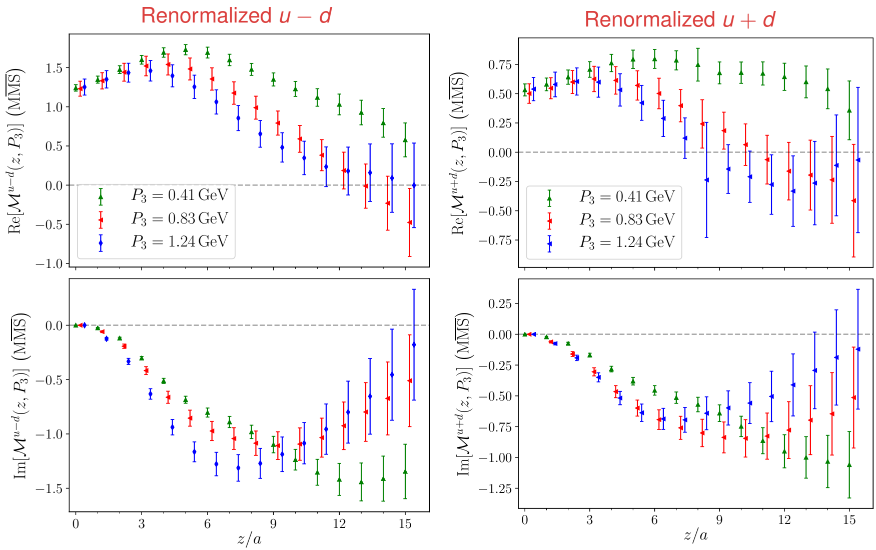

quasi-PDFs and PDFs, light quarks

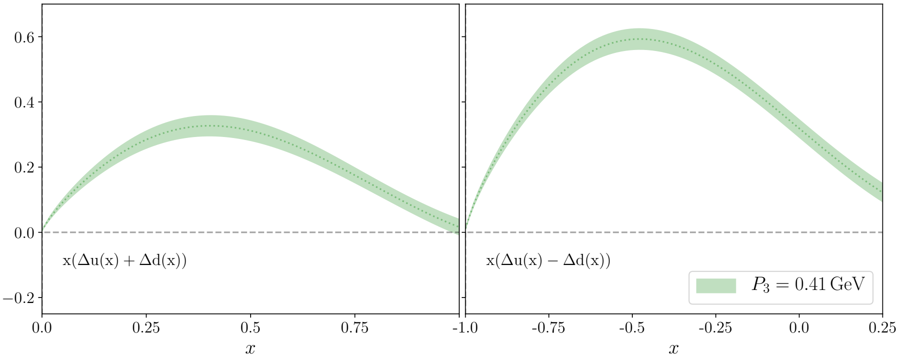

quasi-PDFs and PDFs, light quarks

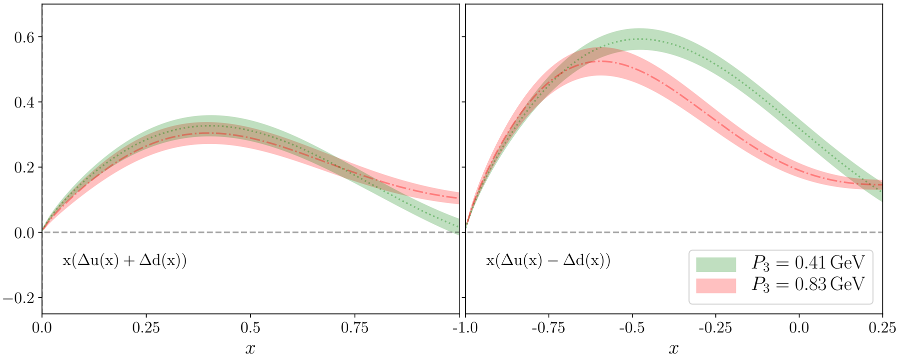

- non-negligible dependence on the momentum going from $P_3 = 0.41\,\mathrm{GeV} \to 0.83\,\mathrm{GeV}$;

quasi-PDFs and PDFs, light quarks

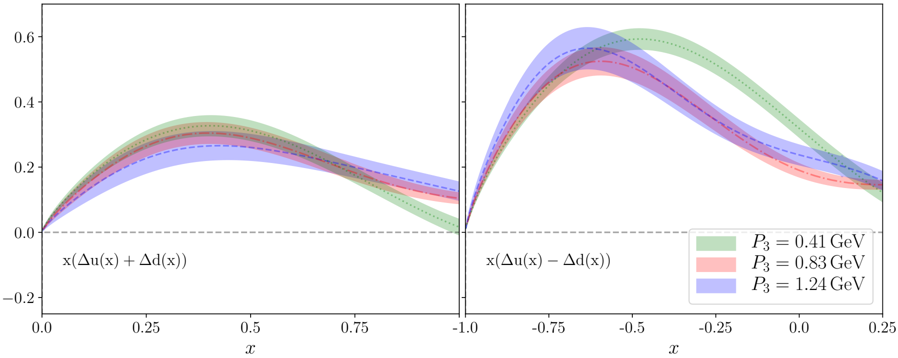

- non-negligible dependence on the momentum going from $P_3 = 0.41\,\mathrm{GeV} \to 0.83\,\mathrm{GeV}$;
- by further increasing the momentum to $P_3 = 1.24\,\mathrm{GeV}$ the distribution remains mostly unaffected;

quasi-PDFs and PDFs, light quarks

Bayes-Gauss-Fourier Transform [Alexandrou et al. (2020) [arXiv:2007.13800v1]

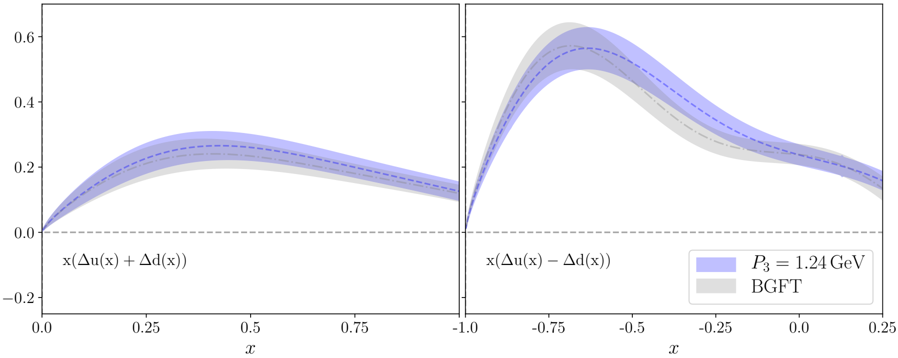

- non-negligible dependence on the momentum going from $P_3 = 0.41\,\mathrm{GeV} \rightarrow 0.83\,\mathrm{GeV}$;
- by further increasing the momentum to $P_3 = 1.24\,\mathrm{GeV}$ the distribution remains mostly unaffected;
- We find agreement between discrete Fourier transform and BGFT $\Rightarrow$ the systematic effect due to the discretization of the FT is negligible.

quasi-PDFs and PDFs, strange

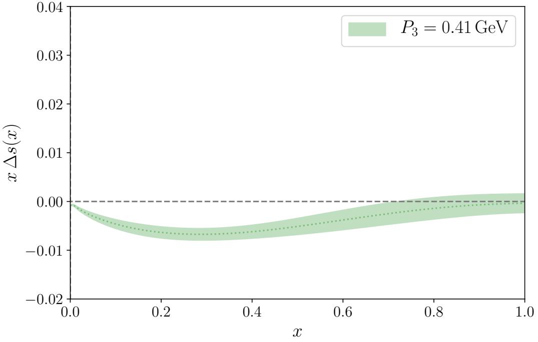

quasi-PDFs and PDFs, strange

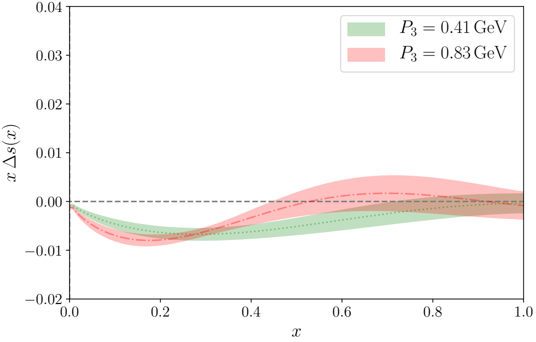

- it decays to zero faster by increasing the nucleon boost;

quasi-PDFs and PDFs, strange

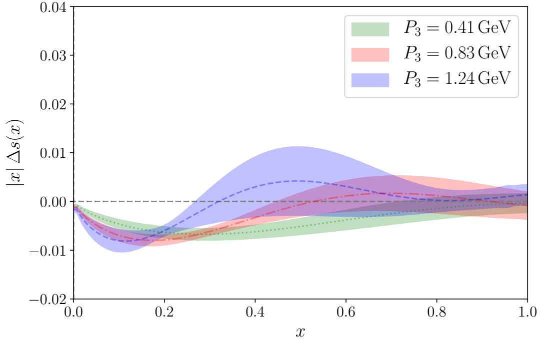

- it decays to zero faster by increasing the nucleon boost;
- it is found compatible with zero at $P_3 = 1.24\,\mathrm{GeV}$ for $x \gtrsim 0.25$;

Systematic effects

Different systematic effects still need to be adressed:

1. pion mass [Alexandrou et al., Phys. Rev. Lett.121,112001 (2018), 1803.02685]

Systematic effects

Different systematic effects still need to be adressed:

1. pion mass [Alexandrou et al., Phys. Rev. Lett.121,112001 (2018), 1803.02685]
2. finite P_3 and t_s
   - the signal exponentially deteriorates with P_3 and with t_s;
   - to take into account the excited stated effect $t_s \gtrsim 1\,\mathrm{fm} \Rightarrow$ at high P_3 this becomes very challenging;
   - momentum smearing effectively helps reducing the signal-to-noise ratio, but the noise still scales exponentially with P_3;

Systematic effects

Different systematic effects still need to be adressed:

1. pion mass [Alexandrou et al., Phys. Rev. Lett.121,112001 (2018), 1803.02685]
2. finite P_3 and t_s
   - the signal exponentially deteriorates with P_3 and with t_s;
   - to take into account the excited stated effect $t_s \gtrsim 1\,\mathrm{fm} \Rightarrow$ at high P_3 this becomes very challenging;
   - momentum smearing effectively helps reducing the signal-to-noise ratio, but the noise still scales exponentially with P_3;
3. cut-off effects

Systematic effects

Different systematic effects still need to be adressed:

1. pion mass [Alexandrou et al., Phys. Rev. Lett.121,112001 (2018), 1803.02685]
2. finite P_3 and t_s
   - the signal exponentially deteriorates with P_3 and with t_s;
   - to take into account the excited stated effect $t_s \gtrsim 1\,\mathrm{fm} \Rightarrow$ at high P_3 this becomes very challenging;
   - momentum smearing effectively helps reducing the signal-to-noise ratio, but the noise still scales exponentially with P_3;
3. cut-off effects
4. truncation of conversion between renormalization schemes and matching
   Two-loops matching [L.-B. Chen et al., 2020, 2005.13757, 2006.10917, 2006.14825]

Systematic effects

Different systematic effects still need to be adressed:

1. pion mass [Alexandrou et al., Phys. Rev. Lett.121,112001 (2018), 1803.02685]
2. finite P_3 and t_s
   - the signal exponentially deteriorates with P_3 and with t_s;
   - to take into account the excited stated effect $t_s \gtrsim 1\,\mathrm{fm} \Rightarrow$ at high P_3 this becomes very challenging;
   - momentum smearing effectively helps reducing the signal-to-noise ratio, but the noise still scales exponentially with P_3;
3. cut-off effects
4. truncation of conversion between renormalization schemes and matching
   Two-loops matching [L.-B. Chen et al., 2020, 2005.13757, 2006.10917, 2006.14825]
5. singlet renormalization and matching

Systematic effects

Different systematic effects still need to be adressed:

1. pion mass [Alexandrou et al., Phys. Rev. Lett.121,112001 (2018), 1803.02685]
2. finite P_3 and t_s
   - the signal exponentially deteriorates with P_3 and with t_s;
   - to take into account the excited stated effect $t_s \gtrsim 1\,\mathrm{fm} \Rightarrow$ at high P_3 this becomes very challenging;
   - momentum smearing effectively helps reducing the signal-to-noise ratio, but the noise still scales exponentially with P_3;
3. cut-off effects
4. truncation of conversion between renormalization schemes and matching
   Two-loops matching [L.-B. Chen et al., 2020, 2005.13757, 2006.10917, 2006.14825]
5. singlet renormalization and matching
6. truncation and discretization of the FT ✓

Systematic effects

Different systematic effects still need to be adressed:

1. pion mass [Alexandrou et al., Phys. Rev. Lett.121,112001 (2018), 1803.02685]
2. finite P_3 and t_s
   - the signal exponentially deteriorates with P_3 and with t_s;
   - to take into account the excited stated effect $t_s \gtrsim 1\,\mathrm{fm} \Rightarrow$ at high P_3 this becomes very challenging;
   - momentum smearing effectively helps reducing the signal-to-noise ratio, but the noise still scales exponentially with P_3;
3. cut-off effects
4. truncation of conversion between renormalization schemes and matching
   Two-loops matching [L.-B. Chen et al., 2020, 2005.13757, 2006.10917, 2006.14825]
5. singlet renormalization and matching
6. truncation and discretization of the FT ✓
7. . . .

Systematic effects

Different systematic effects still need to be adressed:

1. pion mass [Alexandrou et al., Phys. Rev. Lett.121,112001 (2018), 1803.02685]
2. finite P_3 and t_s
   - the signal exponentially deteriorates with P_3 and with t_s;
   - to take into account the excited stated effect $t_s \gtrsim 1\,\mathrm{fm} \Rightarrow$ at high P_3 this becomes very challenging;
   - momentum smearing effectively helps reducing the signal-to-noise ratio, but the noise still scales exponentially with P_3;
3. cut-off effects
4. truncation of conversion between renormalization schemes and matching
   Two-loops matching [L.-B. Chen et al., 2020, 2005.13757, 2006.10917, 2006.14825]
5. singlet renormalization and matching
6. truncation and discretization of the FT ✓
7. ...

To be addressed in the future!

Table of contents

Flavor decomposition

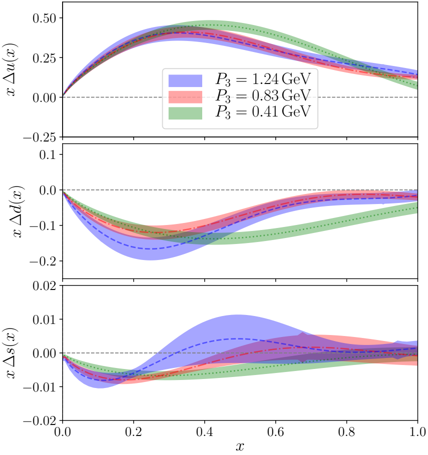

Flavor decomposition

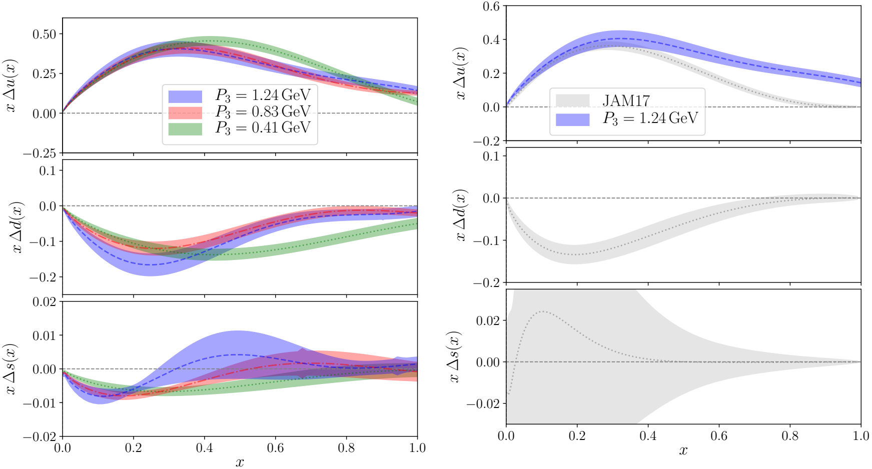

- up quark PDF shows agreement with the global analysis determination in the region $x \lesssim 0.3$;

Flavor decomposition

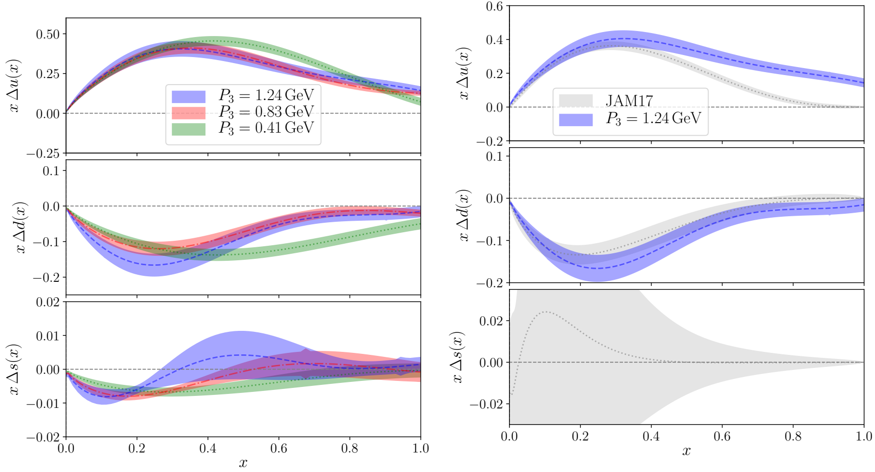

- up quark PDF shows agreement with the global analysis determination in the region $x \lesssim 0.3$;
- for the d-quark we find full agreement with JAM17 phenomenological data;

Flavor decomposition

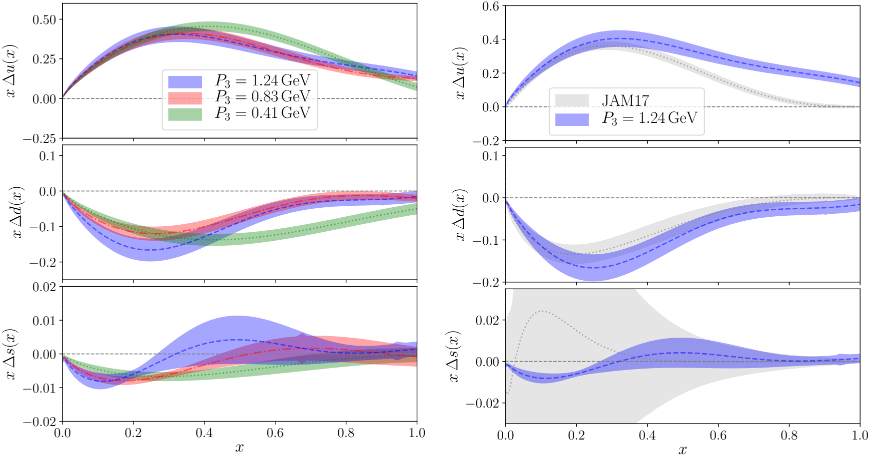

- up quark PDF shows agreement with the global analysis determination in the region $x \lesssim 0.3$;
- for the d-quark we find full agreement with JAM17 phenomenological data;
- our results for Δs are order of magnitudes more precise than global fits, especially in the small x region.

Conclusions

Results obtained so far:

- ☑ Computed renormalized matrix elements for the isoscalar, isovector and s combinations;

Conclusions

Results obtained so far:

- ☑ Computed renormalized matrix elements for the isoscalar, isovector and s combinations;
- ☑ computed the quasi-PDF employing classical discretized Fourier transform and an advanced reconstruction technique;

Conclusions

Results obtained so far:

- ☑ Computed renormalized matrix elements for the isoscalar, isovector and s combinations;
- ☑ computed the quasi-PDF employing classical discretized Fourier transform and an advanced reconstruction technique;
- ☑ performed matching procedure and flavor decomposition;

Conclusions

Results obtained so far:

- ☑ Computed renormalized matrix elements for the isoscalar, isovector and s combinations;
- ☑ computed the quasi-PDF employing classical discretized Fourier transform and an advanced reconstruction technique;
- ☑ performed matching procedure and flavor decomposition;
- ☑ we can obtain Δs with orders of magnitude higher precision compared to phenomenology.

Conclusions

Results obtained so far:

- ☑ Computed renormalized matrix elements for the isoscalar, isovector and s combinations;
- ☑ computed the quasi-PDF employing classical discretized Fourier transform and an advanced reconstruction technique;
- ☑ performed matching procedure and flavor decomposition;
- ☑ we can obtain Δs with orders of magnitude higher precision compared to phenomenology.

the comparison with phenomenological data looks very promising!

Conclusions

Results obtained so far:

- ☑ Computed renormalized matrix elements for the isoscalar, isovector and s combinations;
- ☑ computed the quasi-PDF employing classical discretized Fourier transform and an advanced reconstruction technique;
- ☑ performed matching procedure and flavor decomposition;
- ☑ we can obtain Δs with orders of magnitude higher precision compared to phenomenology.

the comparison with phenomenological data looks very promising!

Future steps:

- ☐ exploratory study of the unpolarized and transversity PDFs;

Conclusions

Results obtained so far:

- ☑ Computed renormalized matrix elements for the isoscalar, isovector and s combinations;
- ☑ computed the quasi-PDF employing classical discretized Fourier transform and an advanced reconstruction technique;
- ☑ performed matching procedure and flavor decomposition;
- ☑ we can obtain Δs with orders of magnitude higher precision compared to phenomenology.

the comparison with phenomenological data looks very promising!

Future steps:

- ☐ exploratory study of the unpolarized and transversity PDFs;
- ☐ in depth evaluation of systematic effects.

Conclusions

Results obtained so far:

- ☑ Computed renormalized matrix elements for the isoscalar, isovector and s combinations;
- ☑ computed the quasi-PDF employing classical discretized Fourier transform and an advanced reconstruction technique;
- ☑ performed matching procedure and flavor decomposition;
- ☑ we can obtain Δs with orders of magnitude higher precision compared to phenomenology.

the comparison with phenomenological data looks very promising!

Future steps:

- ☐ exploratory study of the unpolarized and transversity PDFs;
- ☐ in depth evaluation of systematic effects.

Thank you for your attention!

This project has received funding from the European Union's Horizon 2020 research and innovation programme under grant agreement No 765048.